Local detection of electromagnetic energy transport below the diffraction limit in metal nanoparticle plasmon waveguides

STEFAN A. MAIER*[1], PIETER G. KIK[1], HARRY A. ATWATER[1], SHEFFER MELTZER[2], ELAD HAREL[2], BRUCE E. KOEL[2] AND ARI A.G. REQUICHA[2]

[1]Thomas J. Watson Laboratory of Applied Physics, California Institute of Technology, Mail Stop 128-95, Pasadena, California 91125, USA
[2]Laboratory for Molecular Robotics, Computer Science Department, University of Southern California, Los Angeles, California 90089, USA
*e-mail: stmaier@caltech.edu

Published online: 2 March 2003; doi:10.1038/nmat852

Achieving control of light-material interactions for photonic device applications at nanoscale dimensions will require structures that guide electromagnetic energy with a lateral mode confinement below the diffraction limit of light. This cannot be achieved by using conventional waveguides[1] or photonic crystals[2]. It has been suggested that electromagnetic energy can be guided below the diffraction limit along chains of closely spaced metal nanoparticles[3,4] that convert the optical mode into non-radiating surface plasmons[5]. A variety of methods such as electron beam lithography[6] and self-assembly[7] have been used to construct metal nanoparticle plasmon waveguides. However, all investigations of the optical properties of these waveguides have so far been confined to collective excitations[8–10], and direct experimental evidence for energy transport along plasmon waveguides has proved elusive. Here we present observations of electromagnetic energy transport from a localized subwavelength source to a localized detector over distances of about 0.5 μm in plasmon waveguides consisting of closely spaced silver rods. The waveguides are excited by the tip of a near-field scanning optical microscope, and energy transport is probed by using fluorescent nanospheres.

The transport of electromagnetic energy in plasmon waveguides consisting of closely spaced metal nanoparticles relies on near-field coupling between surface plasmon–polariton modes of adjacent particles. This type of guiding due to near-field coupling has recently been demonstrated experimentally in macroscopic analogues operating in the microwave regime[6,11]. At the submicrometre scale, plasmon waveguides were theoretically and numerically analysed, allowing for the investigation of inter-particle interactions[3], and the dispersion relation and group velocity for energy transport[4]. The characteristics of optical-pulse propagation in plasmon waveguides consisting of spherical or spheroidal nanoparticles were determined by using finite-difference time-domain simulations[12]. Far-field polarization spectroscopy experiments on ordered two-dimensional arrays of Au and Ag nanoparticles with submicrometre inter-particle spacing have confirmed that electromagnetic interactions between the particles are present, revealing energy shifts of the collective plasmon resonances of the particle arrays that are dependent on inter-particle distances[13,14]. It has further been shown that the resonance energy shifts that occur in one-dimensional arrays consisting of closely spaced Au particles enable estimation of the group velocity and energy attenuation length of

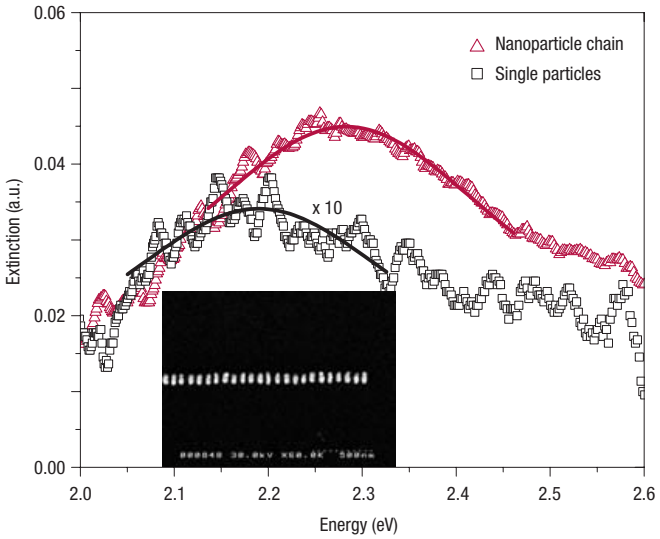

Figure 1 Far-field extinction spectrum of Ag nanoparticle chains and single particles. The far-field extinction spectrum of a plasmon waveguide consisting of Ag nanorods with a 3:1 aspect ratio and a surface-to-surface spacing of 50 nm between adjacent particles shows a plasmon resonance peak shift to higher energies (red triangles and Lorentz fit) compared with the extinction spectrum of isolated, non-interacting particles (black squares and Lorentz fit). The exciting light was polarized along the long axis of the nanorods, perpendicular to the particle chain axis. The inset shows a scanning electron micrograph of the plasmon waveguide layout under study.

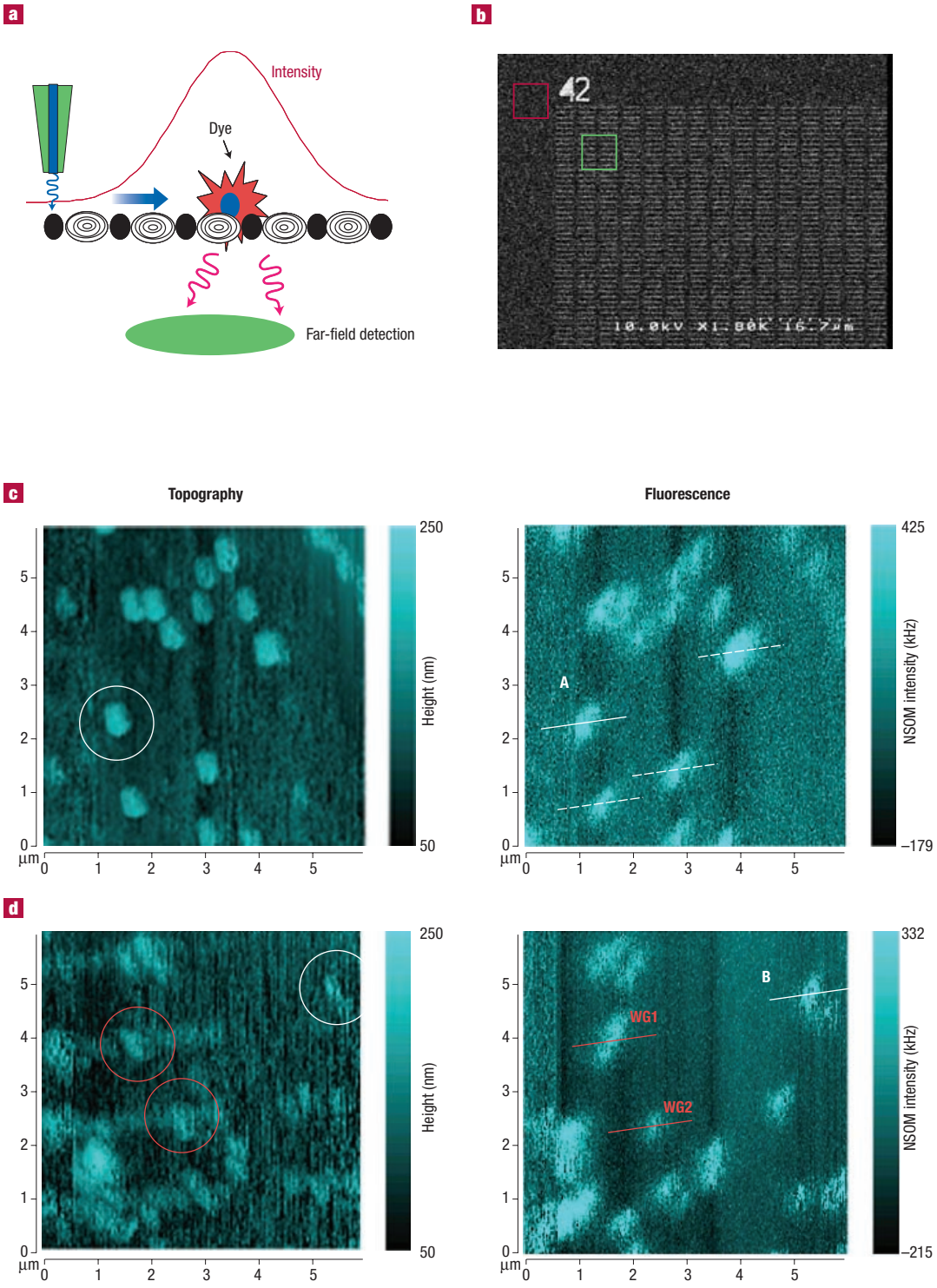

Figure 2 Excitation and detection of energy transport in plasmon waveguides by near-field optical microscopy. a, Sketch of the experiment. Light emanating from the tip of an illumination-mode near-field scanning optical microscope (NSOM) locally excites a plasmon waveguide. The waveguide transports the electromagnetic energy to a fluorescent nanosphere, and the fluorescence intensity for varying tip positions is collected in the far-field. **b**, Scanning electron micrograph of a 100 µm × 100 µm grid consisting of Ag plasmon waveguides. **c**, **d**, Topography and fluorescent NSOM scan of a 6 µm × 6 µm area consisting of single fluorescent nanospheres (**c**, area highlighted by red box in **b**) and an area containing isolated fluorescent nanospheres in the vicinity of plasmon waveguides (**d**, area highlighted by green box in **b**). The fluorescent intensity of two single nanospheres (grey circles and data cuts A and B) can be compared with the intensity distribution of nanospheres on top of plasmon waveguides (red circles, data cuts WG1 and WG2) by using cuts (grey and red lines) through the fluorescent intensity scan along the waveguide axis.

plasmon waveguides[9,10]. Energy attenuation lengths of 6 dB per 30 nm were predicted for plasmon waveguides consisting of closely spaced spherical Au nanoparticles on an indium tin oxide (ITO) substrate. Also, it was shown that a geometry change to spheroidal Ag particles should allow for an attenuation length increase to about 6 dB per 250 nm (ref. 10). This kind of attenuation length is sufficient to allow detection of energy transport by local excitation.

Plasmon waveguides were fabricated by using electron-beam lithography with lift-off on ITO-coated quartz slides, which allowed for a good control over particle size and spacing. The waveguide structures consist of rod-shaped Ag nanoparticles with dimensions of 90 nm × 30 nm × 30 nm and a surface-to-surface spacing of 50 nm between adjacent particles. The long axes of the individual nanoparticles were oriented perpendicular to the waveguide chain axis to allow for an increased near-field coupling between the particles[10]. The inset of Fig. 1 shows a scanning electron micrograph of one of these plasmon waveguides. To allow for the determination of the plasmon resonances of the fabricated structures with a high signal-to-noise ratio using far-field spectroscopy, many plasmon waveguides were arranged in a 100 μm × 100 μm grid with a grating constant of 1 μm as depicted in Fig. 2b. It has previously been shown that cross talk between different waveguides is negligible for this grating constant[9,15]. Thus, far-field extinction spectra on these arrays reflect the properties of individual plasmon waveguides and provide a probe of the near-field coupling between the nanoparticles composing each waveguide.

Figure 1 shows the far-field extinction spectrum of the fabricated plasmon waveguides taken under normal-incidence white-light illumination with a spot size of 100 μm and a polarization along the long axis of the nanoparticles and thus perpendicular to the waveguide-chain axis (red triangles). The extinction spectrum of a grid of single Ag nanoparticles of the same geometry with an inter-particle spacing of 1 μm is also shown, for which the inter-particle coupling is negligible (black squares). The single-particle extinction spectrum peaks at 2.18 eV for a polarization along the long particle axis, corresponding to a resonance wavelength of 570 nm. The extinction spectrum of the plasmon waveguide shows a resonance shift of about 100 meV to higher energies because of near-field coupling between the particles, in agreement with theoretical and numerical studies of aggregated noble-metal nanoparticles[16] and plasmon waveguides[4,12]. According to numerical simulations, this resonance shift of 100 meV translates into a maximum energy attenuation length of the order of 6 dB per 200 nm for an excitation at the single-particle resonance (2.18 eV in these samples), at which the energy transfer in a plasmon waveguide is predicted to be most efficient, independent of inter-particle spacing[4,12].

To probe energy transport directly in the fabricated plasmon waveguides, local excitation is necessary as opposed to far-field excitation of all particles in the arrays. To accomplish this, the tip of an illumination mode near-field scanning optical microscope (NSOM) (Nanonics NSOM-100) (ref. 17) is used as a local excitation source for nanoparticles in plasmon waveguides. To excite the mode of least damping, laser light from a dye laser at a wavelength of 570 nm, corresponding to the single-particle resonance, was coupled into a multi-mode optical fibre attached to the Al-coated NSOM tip used for excitation. Figure 2a shows a schematic of our approach to excitation and energy transport detection. Power transport away from the directly excited nanoparticles in the plasmon waveguide is probed by the placement of carboxyl-coated polystyrene nanospheres (Molecular Probes Fluospheres F-8801, diameter 110 ± 8 nm) filled with fluorescent molecules[18] in close proximity to the waveguide structure. For this, the electron-beam-fabricated plasmon waveguide sample was coated with a thin polylysine layer, and the nanospheres were subsequently randomly deposited from an aqueous solution. The fluorescent dyes used show a strong absorption, peaking at 580–590 nm near the plasmon resonance wavelength of a single fabricated Ag particle and having their emission maximum at 610 nm. The excitation light was

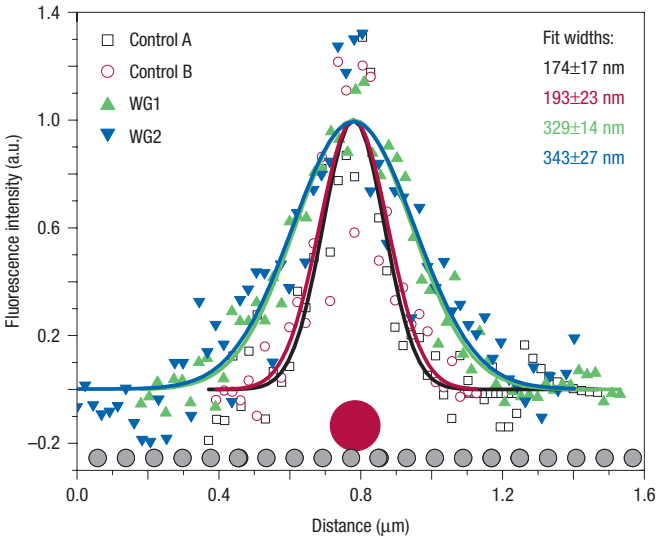

Figure 3 Evidence for energy transport in plasmon waveguides by the width of the intensity of fluorescent nanospheres. Individual data sets represent averages of five parallel cuts along the plasmon waveguide direction through the fluorescent spots highlighted in Fig. 2c, d for isolated nanospheres (control A and B, black and red data points) and nanospheres located on top of plasmon waveguides (WG 1 and WG2, green and blue data points) as depicted in the inset. Gaussian line-shape fits to the data show an increased width for nanospheres located on plasmon waveguides.

filtered out by using a band-pass filter, and the 610 nm dye emission was detected in the far-field with an avalanche photo diode. This scheme enables the observation of energy transport in the following way: first, energy is transferred from the illuminating tip to the plasmon waveguide. The excitation subsequently propagates along the nanoparticle structure and excites a fluorescent nanosphere placed on top of a waveguide at a sufficient distance from the excitation source. Energy transport would result in dye emission even when the microscope tip is located away from the dye, and thus would manifest itself in an increased spatial width of the fluorescence spot of a nanosphere attached to a plasmon waveguide compared with a single free nanosphere.

Figure 2c,d shows simultaneously obtained topography and fluorescent NSOM scans of the control area outside the grid (Fig. 2b, red box) with single nanospheres only and of the plasmon waveguide grid (Fig. 2b, green box) together with fluorescent nanospheres, respectively. The samples were illuminated at the single-particle resonance wavelength of 570 nm by using a microscope tip with a 100 nm aperture. The scans were done in constant gap mode, ensuring a fixed vertical distance between the exciting tip and the fluorescent nanospheres both for isolated spheres and for spheres located on plasmon waveguides. The scan direction was perpendicular to the plasmon waveguides, and images were built up from left to right. Figure 2c shows a scan of a control area consisting of single nanospheres only, which was taken immediately before scanning the plasmon waveguide area. Single nanospheres are clearly resolved in both the topography and the fluorescent NSOM image. Intensity variations are observed between different fluorescent nanospheres, which are attributed to slight variations in the nanosphere diameter; the elongation of the fluorescent spots is due to a tip artefact. Figure 2d shows the subsequent scan of a sample area comprising four plasmon waveguides in the left part of the image and fluorescent nanospheres. Two nanospheres (highlighted by red circles) are located on top of plasmon waveguides, and one

nanosphere at the right side of the scan area (grey circle) is positioned at a distance from a waveguide structure and can thus serve as a further control to ensure that tip characteristics do not change during the scans. The widths of the fluorescence spots of several control nanospheres of Fig. 2c,d and of the nanospheres attached to waveguides of Fig. 2d were examined by taking cuts through the microscope data parallel to the plasmon waveguide direction, as highlighted in the fluorescent images (red and grey lines).

Figure 3 shows averages of five parallel cuts through fluorescent nanosphere spots A, B, WG1 and WG2. Gaussian fits to the data for both the control spheres (black and red lines and data points) and the two spheres attached to plasmon waveguides (green and blue lines and data points) are included. The control nanospheres A and B were scanned before and after scanning the waveguide structures, and in both cases show similar fluorescent full-widths at half maximum (FWHM) of 174 ± 17 and 193 ± 23 nm. Analyses of additional control spheres (indicated by dashed grey lines in Fig. 2c) yielded similar widths of 160 ± 12, 205 ± 13 and 188 ± 17 nm, respectively. This confirms that the tip profile did not change appreciably during the scans. By contrast, the fluorescent spots WG1 and WG2 of the nanospheres attached to the plasmon waveguides show a FWHM of 329 ± 14 and 343 ± 27 nm, respectively. The resulting average fluorescence spot FWHM of control spheres was 185 ± 38 nm, whereas the average width of nanospheres on waveguides was 336 ± 30 nm. The broadening of the fluorescence spots caused by the presence of the plasmon waveguide was thus 151 ± 48 nm.

If the observed broadening of the fluorescent width of waveguide nanospheres is due to transport of electromagnetic energy along the waveguide, no difference in FWHM between control and waveguide nanospheres is expected in the direction perpendicular to the waveguide axis. Indeed, the fitted FWHMs in this direction are found to be equal within the fit error, giving 364 ± 36 nm for control A and B and 352 ± 40 nm for the waveguide nanospheres WG1 and WG2. Note that these values are rather large because of the shape of the tip aperture (see microscope scans in Fig. 2).

The increase in the width of the nanosphere fluorescence of about 150 nm for spheres attached to a plasmon waveguide structure can be attributed to local excitation of the plasmon waveguide followed by energy transport along the waveguide towards the fluorescent dye particle. This type of excitation is known to dominate over excitation by direct scattering of the exciting radiation from individual nanoparticles[12]. From Fig. 3 it is clear that for a free-standing nanosphere the fluorescence signal decreases below the dark noise level if the tip is located approximately 200 nm away from the sphere centre, whereas a fluorescent nanosphere attached to a plasmon waveguide can be excited from distances up to 500 nm by the plasmon waveguide. Our results thus provide direct evidence for energy transport over this distance. To obtain quantitative information on the energy decay length we have performed exponential fits on the tails of the fluorescence intensity of the waveguide nanospheres at distances greater than 200 nm away from the nanosphere centre. At this distance, excitation by the plasmon waveguide dominates over direct dye excitation. These fits yield a decay length of 6 dB per 195 ± 28 nm, which is in excellent agreement with the estimate of 6 dB per 200 nm obtained from our far-field measurements and theoretical predictions.

An energy attenuation length of several hundred nanometres suggests the use of plasmon waveguides as functional end-structures in integrated optical devices. Further improvements to the inter-particle coupling and the use of low-loss substrates should allow for the fabrication of plasmon waveguides with larger energy-attenuation lengths, and thus enable numerous applications for light-guiding and light-focusing elements operating below the diffraction limit.

Received 9 December 2002; accepted 29 January 2003; published 2 March 2003.

References

1. Saleh, B. E. A. & Teich, M. C. *Fundamentals of Photonics* (Wiley, New York, 1991).
2. Mekis, A. *et al.* High transmission through sharp bends in photonic crystal waveguides. *Phys. Rev. Lett.* **77,** 3787–3790 (1996).
3. Quinten, M., Leitner, A., Krenn, J. R. & Aussenegg, F. R. Electromagnetic energy transport via linear chains of silver nanoparticles. *Opt. Lett.* **23,** 1331–1333 (1998).
4. Brongersma, M. L., Hartman, J. W. & Atwater, H. A. Electromagnetic energy transfer and switching in nanoparticle chain arrays below the diffraction limit. *Phys. Rev. B* **62,** R16356 (2000).
5. Kreibig, U. & Vollmer, M. *Optical Properties of Metal Clusters* (Springer, Berlin, 1995).
6. Maier, S. A. *et al.* Plasmonics – a route to nanoscale optical devices. *Adv. Mater.* **13,** 1501–1505 (2001).
7. McMillan, R. A. *et al.* Ordered nanoparticle arrays formed on engineered chaperonin protein templates. *Nature Mater.* **1,** 247–252 (2002).
8. Krenn, J. R. *et al.* Squeezing the optical near-field zone by plasmon coupling of metallic nanoparticles. *Phys. Rev. Lett.* **82,** 2590–2593 (1999).
9. Maier, S. A., Brongersma, M. L., Kik, P. G. & Atwater, H. A. Observation of near-field coupling in metal nanoparticle chains using far-field polarization spectroscopy. *Phys. Rev. B* **65,** 193408 (2002).
10. Maier, S. A., Kik, P. G. & Atwater, H. A. Observation of coupled plasmon–polariton modes in Au nanoparticle chain waveguides of different lengths: Estimation of waveguide loss. *Appl. Phys. Lett.* **81,** 1714–1716 (2002).
11. Maier, S. A., Brongersma, M. L. & Atwater, H. A. Electromagnetic energy transport along arrays of closely spaced metal rods as an analogue to plasmonic devices. *Appl. Phys. Lett.* **78,** 16–18 (2001).
12. Maier, S. A. *et al.* Optical-pulse propagation in metal nanoparticle chain waveguides. *Phys. Rev. Lett.* (submitted).
13. Lamprecht, B. *et al.* Metal nanoparticle gratings: influence of dipolar particle interaction on the plasmon resonance. *Phys. Rev. Lett.* **84,** 4721–4724 (2000).
14. Salerno, M., Felidj, N., Krenn, J. R., Leitner, A. & Aussenegg, F. R. Near-field optical response of a two-dimensional grating of gold nanoparticles. *Phys. Rev. B* **63,** 165422 (2001).
15. Schider, G. *et al.* Optical properties of Ag and Au nanowire gratings. *J. Appl. Phys.* **90,** 3825–3830 (2001).
16. Quinten, M. & Kreibig, U. Absorption and elastic scattering of light by particle aggregates. *Appl. Opt.* **32,** 6173–6182 (1993).
17. Lieberman, K., Ben-Ami, N. & Lewis, A. A fully integrated near-field optical, far-field optical, and normal-force scanned probe microscopy. *Rev. Sci. Instrum.* **67,** 3567–3572 (1996).
18. Fujihira, M. *et al.* Scanning near-field optical microscopy of fluorescent polystyrene spheres with a combined SNOM and AFM. *Ultramicroscopy* **61,** 271–277 (1995).

Acknowledgements

The authors are grateful to Richard Muller, Paul Maker, and Pierre Echternach of the Jet Propulsion Laboratory in Pasadena for professional help with electron beam lithography. This work was sponsored by the Air Force Office of Scientific Research and also partly by the NSF grants ECS0103543, EIA-98-71775 and DMI-02-09678 and the Center for Science and Engineering of Materials at Caltech. Correspondence and requests for materials should be addressed to S.M.

Competing financial Interests

The authors declare that they have no competing financial interests.